(2) A transition to a state at about 2.06 MeV is the strongest radiation from the two $J=0$ capturing states, but is much weaker from the two $J=1$ states.

(3) There are four "allowed" (i.e., $E1$) transitions from capturing states to the possible "two-phonon" levels at 1.27, 1.05, and 0.95 MeV. Two of these transitions are of moderate strength and two are very weak —in fact, too weak to be detected. Thus, these results indicate some, but not complete, inhibition of transitions from the capturing state to the possible "two-phonon" states, as compared with transitions to frequently populated states at higher excitation energies (say, the 1.57-MeV state mentioned above).

(4) The two allowed transitions to the "one-phonon" 0.37-MeV state have about the same strength as the transitions to the "two-phonon" states.

ACKNOWLEDGMENT

The authors wish to thank the various members of the chopper group for their assistance throughout this work.

PHYSICAL REVIEW VOLUME 133, NUMBER 3B 10 FEBRUARY 1964

States in Si^{28} with $12.7<E_x<13.7$ MeV by (α,γ) and (α,α) Reactions on Mg^{24}†

J. A. WEINMAN, L. MEYER-SCHÜTZMEISTER, AND L. L. LEE, JR.
Argonne National Laboratory, Argonne, Illinois

(Received 20 September 1963)

The radiative capture and elastic scattering of alpha particles by Mg^{24} have been studied for alpha-particle energies between 3.2 and 4.5 MeV. The yield and angular distributions of the gamma radiation in combination with a dispersion analysis of the $Mg^{24}(\alpha,\alpha)Mg^{24}$ data gave information on the resonance energies, angular momenta, parities, and some partial widths of states in Si^{28}. The excitation energies and the corresponding spins and parities of the Si^{28} levels considered were: 12.74 MeV, 2^+; 12.82 MeV, [0^+ or 3^-]; 12.83 MeV, 1^-; 12.87 MeV, 4^+; 12.92 MeV, 2^+; 12.99 MeV, 1^- and 0^+ (two levels); 13.06 MeV, 0^+; 13.12 MeV, 2^+; 13.19 MeV, [?]; 13.25 MeV, 0^+; 13.27 MeV, [1^-]; 13.38 MeV, [?]; and 13.71 MeV, 2^+.

I. INTRODUCTION

THE simple features of alpha-particle capture by a zero-spin nucleus often warrant a unique assignment of spins and parities to the energy levels of the compound nucleus. In cases in which the assignment is not unambiguous, measurements of elastic α-particle scattering can help to determine the parameters of excited states. The (α,γ) and (α,α) processes in Mg^{24} are therefore promising for investigating the Si^{28} nucleus.

Theoretical descriptions of the states of Si^{28} are quite difficult and unreliable for all but the lowest excited states.[1] However, the levels of Si^{28} at excitation energies above 11 MeV have been extensively studied by experiment, chiefly by the reactions $Al^{27}(p,\gamma)Si^{28}$,[2] $Al^{27}(p,\alpha)Mg^{24}$,[3] $Mg^{24}(\alpha,p)Al^{27}$, and $Mg^{24}(\alpha,\alpha)Mg^{24}$.[4] Recently, Smulders and Endt[5] have reported measurements on $Mg^{24}(\alpha,\gamma)Si^{28}$ with alphas incident at energies up to 3.22 MeV; the Si^{28} was excited to states between 11.30 and 12.74 MeV. This paper reports results extending the study of this reaction to 13.7-MeV excitation in Si^{28}.

II. EQUIPMENT

In the early stages of the experiment the capture gamma radiation was detected by a 4×4-in. NaI crystal. For later studies of all the weaker resonances, the detection was considerably improved through the use of a NaI crystal 10 in. in diameter and 8 in. long. Both crystals were mounted on an arm which could easily be rotated about the target spot and on which the detector-target distance could easily be adjusted. The initial optical alignment was checked by the necessary symmetries of the capture gamma rays.

Enriched Mg^{24} targets[6] evaporated *in situ* on tantalum backings were bombarded with an α-particle beam from the Argonne 4.5-MeV Van de Graaff generator. The special arrangement used to minimize carbon contamination on the target and to permit intense beams is described elsewhere.[7] Whenever a high-energy resolution (an energy spread of less than 1 keV in the beam) was required, the α particles passed through a 90° electrostatic analyzer with a radius of 1 m. Although

† Work performed under the auspices of the U. S. Atomic Energy Commission.

[1] A. V. Cohen and J. A. Cookson, Nucl. Phys. **29**, 604 (1961).

[2] S. L. Anderson, H. Bö, T. Holtebekk, O. Lønsjø, and R. Tangen, Nucl. Phys. **9**, 509 (1959). The work of these and other authors has been summarized by A. M. Endt and C. Van der Leun, Nucl. Phys. **34**, 1 (1962).

[3] S. L. Anderson, A. Haug, T. Holtebekk, O. Lønsjø, and R. Nordhagen, Physica Norvegica **1**, 1 (1961).

[4] S. G. Kaufmann, E. Goldberg, L. J. Koester, and F. P. Mooring, Phys. Rev. **88**, 673 (1952).

[5] P. J. M. Smulders and P. M. Endt, Physica **28**, 1093 (1962).

[6] Obtained from Oak Ridge National Laboratory.

[7] J. A. Weinman, Nucl. Instr. Methods (to be published).

relative α-particle energies could be determined with an error less than 2 keV, we did not make a precise absolute energy determination. Instead, all of our energies are established relative to the prominent 2^+ resonance at $E_\alpha = 3.213$ MeV studied by other workers.[8]

For the elastic scattering studied, the analyzed beam entered a 20-cm scattering chamber of conventional design. The energy spread of the incident beam was always much less than the observed target thickness. The enriched Mg^{24} was evaporated onto thin carbon backings and the yield of elastically scattered α particles was measured over the energy range $3.2 \leqslant E_\alpha \leqslant 3.9$ MeV. The scattered alpha particles were detected in several solid-state counters placed at angles $\theta_{c.m.} = 149.5°$, 140.8°, 125.4°, and 90° (corresponding to zeros of the Legendre polynomials with $l = 4$, 3, 2, and 1, respectively), and at a back angle of 167.1°.

III. MEASUREMENTS

A. Excitation Functions, Total Widths, and γ-Ray Spectra

For the measurement of excitation functions, single-channel analyzers were set so that gamma rays whose pulse heights corresponded to transitions to the ground state and to the first excited state of Si^{28} were counted separately. The yields of these two gamma rays at 45° to the beam are shown as a function of alpha-particle energy in Fig. 1. To get maximum efficiency, the crystal

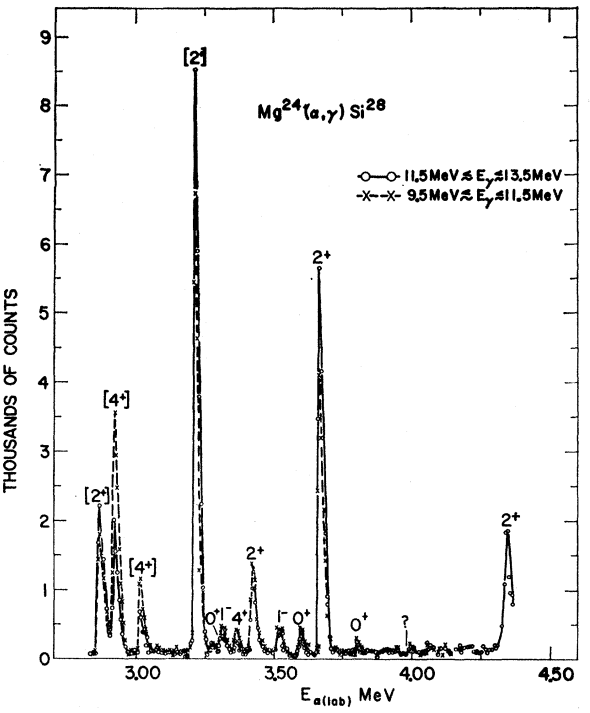

FIG. 1. Yield of high-energy gamma rays from alpha-particle bombardment of Mg^{24}, plotted as a function of alpha-particle energy. For all resonances above 3.2-MeV alpha energy, the spins and parities indicated are those listed in Table I. The values enclosed in square brackets have been measured by other workers.

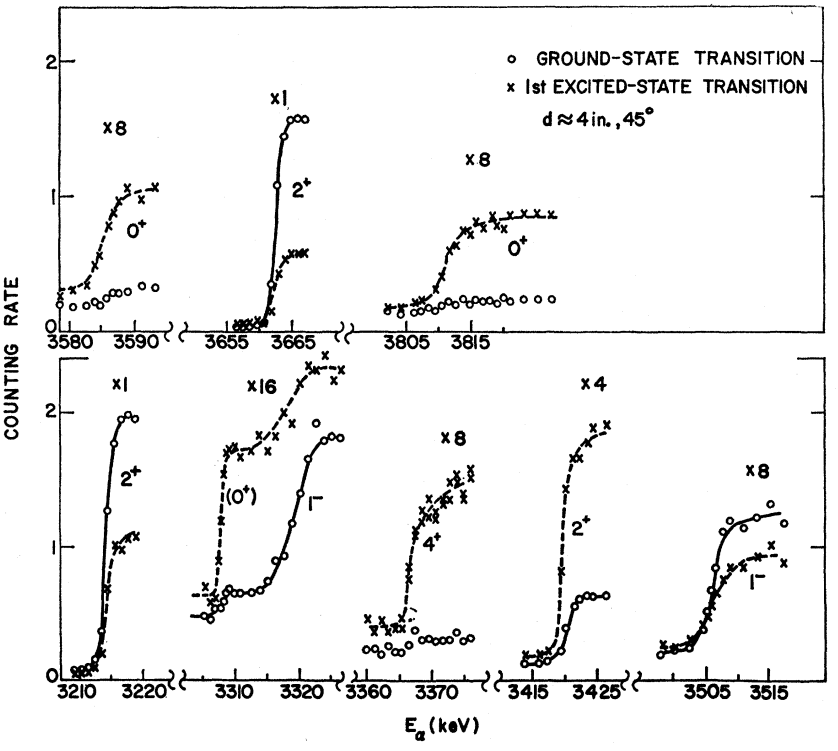

FIG. 2. "Thick target" yield curves for eight prominent resonances. The gamma rays were detected in a NaI crystal 8 in. deep by 10 in. in diameter, placed 4 in. from the target and at 45° to the beam direction. In order to depict all resonances on the same scale, the actual counting rates have been multiplied by the number indicated for each resonance. The energy spread in the beam was 1 keV or less. Spin and parity assignments are those listed in Table I.

[8] The value used here is given by Endt and Van der Leun in their review paper [Nucl. Phys. 34, 1 (1962)]. A precision measurement $E_\alpha = 3199.8 \pm 1.0$ keV has been reported by A. Rytz, H. H. Staub, H. Winkler, and F. Zamboni, Helv. Phys. Acta 35, 546 (1962). Our values can be adjusted to this newer value by a suitable subtraction.

TABLE I. Experimental results of the $Mg^{24}(\alpha,\gamma)Si^{28}$ and $Mg^{24}(\alpha,\alpha)Mg^{24}$ reactions. For comparison, the values of other authors are given.

E_α(lab) (MeV)	E_x[a] (MeV)	I^π (α,γ)	I^π (α,α)	I^π (p,α)[b]	Γ_T (keV) (α,α)	Γ_T (keV) (α,γ)	Γ_T (keV) (p,γ)[c]	Γ_α/Γ_T (α,α)	$(2I+1)\Gamma_p\Gamma_\alpha/\Gamma_T$ (eV)	Γ_α (keV)	Γ_p (keV)	$(2I+1)\Gamma_\alpha\Gamma_\gamma/\Gamma$ (eV) g.s.	$(2I+1)\Gamma_\alpha\Gamma_\gamma/\Gamma$ (eV) exc.	Γ_γ (eV) measured g.s.	Γ_γ (eV) measured exc.	Γ_γ (eV) calculated g.s.	Γ_γ (eV) calculated exc.
3.213	12.740	2^+	2^+	2^+	1.1 ± 0.3	0.8 ± 0.5	0.710 ± 0.130	0.4 ± 0.2	940	0.42[d]	0.34[d]	4.6	1.5	2.3	0.75	1.38(E2)	0.65(E2)
3.307	12.820	$(0^+,3^-)$	[e]	[f]		$\leqslant 0.6$	<0.200		1.7			<0.02	0.18				
3.318	12.830	1^-	1^-	[f]	$2.0^{+0.6}_{-0.3}$	2.8 ± 0.5		0.7 ± 0.1	3.4	2.0 ± 0.4	0.0016 ± 0.0002	0.26	<0.04	0.13		1320(E1)	
3.363	12.869	4^+	[e]	4^+		$\leqslant 0.6$	<0.160		35			<0.02	0.09				
3.418	12.919	2^+	2^+	2^+	0.7 ± 0.3	1.3 ± 0.5	~ 1.100	0.3 ± 0.2	1640	0.6[b]	0.6[b]	0.14	0.86	0.17	0.57	1.48(E2)	0.71(E2)
3.447	12.941	[e]	[e]	$(2^+,3^-)$		[e]	0.290 ± 0.070		206								
3.504	12.989	1^- [e]	(1^-) 0^+		$\geqslant 2.9$	1.5 ± 0.5		$\lesssim 0.5$	<860	$\geqslant 2.9$	$\leqslant 1.7$	0.29	0.04				
3.583	13.056	(0^+)	0^+		$2.2^{+0.8}_{-0.4}$	2.4 ± 0.5		0.9 ± 0.1	<40	2.2 ± 0.4	$\leqslant 0.05$	<0.02	0.22		0.2		0.75(E2)
3.660	13.123	2^+	(2^+)			0.8 ± 0.5		0.8 ± 0.2				3.4	$\lesssim 0.3$	0.85		1.59(E2)	
3.737	13.189	[e]	[f]			[e]											
3.807	13.249	(0^+)	0^+		$\geqslant 2.1$	2.3 ± 0.6		0.9 ± 0.1	<580	2.1 ± 0.4	<0.73	<0.03	0.14		0.13		0.82(E2)
3.827	13.266	[e]	(1^-)			[e]		[f]									
3.961	13.381	[f]				3.0 ± 0.7											
4.349	13.714	2^+															

[a] Computed on the assumption that $Q_0 = 9.986$ MeV.
[b] From Anderson *et al.*, Ref. 3.
[c] From Anderson *et al.*, Ref. 2.
[d] From P. J. M. Smulders (private communication).
[e] Not observed.
[f] Not measured although resonance observed.

was placed as close to the target as possible—about 4 in. At this close distance, the simultaneous absorption of both gamma rays from a two-step transition to the ground state led to pulses that simulated a true ground-state transition. This contribution is included in the data shown by circles in Fig. 1; it is revealed most clearly at the 0^+ and 4^+ resonances for which there is no direct ground-state transition at all. The dashed curve includes the photopeak for the first excited-state transition but, of course, also includes a contribution from the tail of the higher energy gamma ray. Spin and parity could be assigned to many of the resonances shown in Fig. 1; the assignments indicated in brackets have already been published by others.

The two very close 0^+ and 1^- levels at 3.31 MeV, and the widths of these and the other resonances, were studied in more detail with the higher energy resolution obtainable with the 90° electrostatic analyzer. A semithick Mg^{24} target was used. Again the detector was pushed close to the target and placed at an angle of 45° to the direction of the incoming beam. To depict

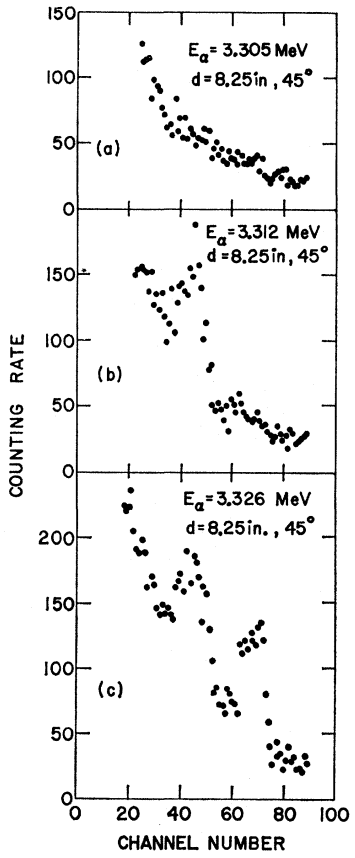

FIG. 3. Uncorrected gamma-ray spectra taken in the region of the 3.307- and 3.318-MeV resonances. The gamma rays were detected in a NaI crystal 8 in. thick by 10 in. in diameter, placed 8.25 in. from the target and at 45° to the incident beam. The three spectra were taken (a) just below both resonances, (b) on the peak of the 3.307-MeV resonance, and (c) on the peak of the 3.318-MeV resonance. Because of target thickness, (c) also includes the contribution of the 3.307-MeV resonance (Fig. 2).

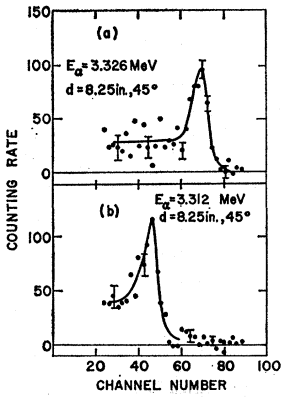

FIG. 4. Spectra shown in Fig. 3 after suitable background subtraction (see text). (a) Spectrum due to 3.318-MeV resonance. (b) Spectrum due to 3.307-MeV resonance.

resonances on the same scale, the actual counting rate was multiplied by the number indicated for each resonance; the result is shown in Fig. 2. As before, the ground-state transition is often only a simulated one resulting from the summation pulses; and again the number of gamma rays with the energy of the transition to the first excited state has been increased by the ground-state transition. Unfortunately, the 4.35-MeV resonance could not be studied with the electrostatic analyzer because of voltage limitations.

The total widths Γ obtained from the measurements in Fig. 2 are listed in Table I for all the resonances. Two resonances near the alpha-particle energy of 3.31 MeV are clearly seen to be separated by 11 keV. They have different widths, and their gamma-ray widths (both $\Gamma_{\gamma 1}$ for the transition to the first excited state and $\Gamma_{\gamma 0}$ to the ground state) are markedly different.

B. Angular Distributions and Absolute γ-Ray Yields

For angular-distribution measurements, the detector surface was pulled back to a distance of 10 in. from the target. The solid angle subtended by the detector then was sufficiently small that the number of summation pulses was greatly decreased—in fact, within the statistical uncertainty from the background, no pulses with energies corresponding to the ground-state transition could be identified at the resonances with 0^+ or 4^+ spin assignments. As an example, the two resonances at about 3.31 MeV are plotted in Figs. 3 and 4 for a distance of 8.25 in. from target to detector.

Figure 3 shows three total gamma-ray spectra. Figure 3(a) shows the result at an alpha-particle energy just below the first of the resonances at 3.305 MeV. There is no indication of a peak near channel 45 or 68 where the transitions to the first excited state and the ground state, respectively, would appear. Instead the counting rate decreases more or less exponentially. This spectrum is attributed to the neutrons produced abundantly in a $C^{13}(\alpha,n)O^{16}$ reaction on a C^{13} contamination of the Mg target. Figure 3(b) shows the gamma-ray spectrum at an energy of 3.312 MeV, just above the 3.307-MeV resonance. To eliminate the background,

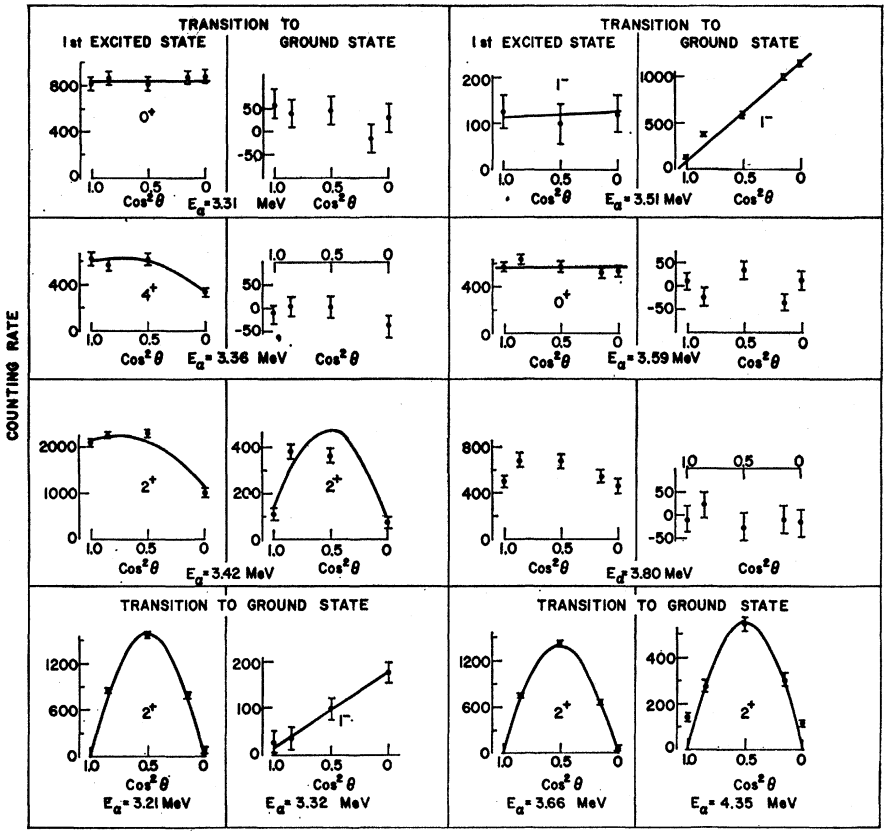

FIG. 5. Gamma-ray angular distributions measured on the peaks of the various resonances studied. Alpha-particle energies and observed transitions (to ground state or excited state) are indicated with each plot. The solid curves are theoretical curves calculated for a resonance having the spin and parity indicated and corrected for finite solid angle of the detector. At the resonance at $E_\alpha=3.42$ MeV, the transition to the first excited state is of mixed multipolarity, the intensity ratio being $I(\mathrm{E2})/I(\mathrm{M1})=4$.

we subtract the gamma-ray spectrum [Fig. 3(a)] below the resonance. The difference is plotted in Fig. 4(b), which clearly exhibits a gamma-ray transition to the first excited state. The gamma-ray intensity at the energy of the ground-state transition is zero within the statistical error. Figure 3(c) is a plot of the gamma-ray spectrum just above the spin-1^- second resonance at 3.326 MeV. The spectrum in Fig. 3(b) was taken as background and subtracted. The result is shown in Fig. 4(a). Here the ground state is predominant and hardly any transition to the first excited state can be seen. The vertical bars indicate the probable statistical error at different energies in the γ-ray spectrum.

For all angular-distribution measurements and for the determination of the absolute gamma-ray yield of the different resonances, the background was determined by taking the gamma-ray spectrum just below the resonance of interest. The background spectrum was then subtracted channel by channel from the gamma-ray spectrum taken at the maximum yield of the resonance.

The absolute gamma-ray yield was measured with a thick Mg target. At each resonance the gamma-ray counting rates of the transitions to the first excited state and to the ground state were measured at a suitable angle. The distance from target to detector was usually 10 in. Only the gamma rays under the peaks in the gamma-ray spectrum were counted and the area of the peak was assumed to represent 50% of the gamma rays falling onto the surface of the crystal. The absolute γ-ray yield Y was then obtained by integrating this number of γ rays over the whole sphere, the angular distribution of the resonance and the correction for the finite solid angle of the detector being taken into account. This yield can be expressed in the form

$$\omega\gamma=(2I+1)(\Gamma_\alpha\Gamma_\gamma/\Gamma)=2\epsilon Y/\lambda^2,$$

where Γ_α, Γ_γ, and Γ are the widths for alpha-particle, gamma-ray, and total emission, λ is the wavelength of the α particle, I is the spin of the compound nucleus, ϵ represents the stopping power of the alpha beam in the target,[9] and $\gamma=\Gamma_\alpha\Gamma_\gamma/\Gamma$. The gamma-ray widths and the expression $\omega\gamma$ for the transitions to the ground state and to the first excited state are listed separately in Table I.

C. Elastic Scattering of α Particles

The targets, magnesium metal enriched to 99.7% Mg^{24}, were evaporated to a thickness of about 0.01 mg/cm² on carbon foils about 0.03 mg/cm² thick. The solid-state counters detected three groups of scattered

[9] W. Whaling, in *Handbuch der Physik*, edited by S. Flügge (Springer Verlag, Berlin, 1958), Vol. 34, p. 193.

α particles whose energies indicated that they were scattered from C, O, and Mg. A blank backing indicated the presence of C only. The abundance ratio $Mg^{24}/O^{16} = 0.85$ was obtained by observing the yields of the $Mg^{24}(\alpha,\alpha)Mg^{24}$ and of $O^{16}(\alpha,\alpha)O^{16}$ reactions under identical circumstances and comparing these with their respective absolute cross sections. The cross section of O^{16} has been measured[10]; for Mg^{24} the absolute cross section at 90° was calculated by assuming only Rutherford scattering in the nonresonant energy region. The $Mg^{24}(\alpha,\alpha)Mg^{24}$ cross section at angles other than 90° was derived from the relative yield of α particles elastically scattered from Mg^{24} and O^{16} and the derived abundance ratio. These calculated cross sections were consistent within 10% with the assumption that only the Rutherford scattering is important for the nonresonant energy region studied in $Mg(\alpha,\alpha)Mg$. A target thickness of about 13 keV was calculated by assuming that O^{16} and Mg^{24} is distributed uniformly in the target. (Since these targets were about 13 keV thick for 3.5-MeV alpha particles, it was impossible to observe resonances having total widths less than about 500 eV.[11])

IV. RESULTS

The measured excitation function and the thick-target yield curves used in obtaining total widths have been cited earlier and are shown in Figs. 1 and 2. Angular distributions measured at the various (α,γ) resonances studied are shown in Fig. 5, in which the solid lines are theoretical curves calculated for the indicated transitions and corrected for the finite solid angle subtended by the gamma detector.[12] Quite good fits can usually be obtained.

The results of the elastic-scattering measurements are displayed in Fig. 6, which shows the excitation functions measured at the five angles cited earlier. The elastic-scattering results do not cover the entire energy range of the (α,γ) experiment; they were ordinarily used only to resolve ambiguities. The measurements at 167° agree quite well with those of previous investigators.

V. DISCUSSION

In the alpha-particle capture by a zero-spin nucleus such as Mg^{24}, only states with spins and parities 0^+, 1^-, 2^+, 3^-, 4^+, etc. can be excited in Si^{28}. Of these, only the 1^- and 2^+ states are able to decay directly to the 0^+ ground state. Whenever one of these transitions is observed, the angular distribution of its gamma rays reveals the spin assignment of the excited Si^{28} level uniquely.

In contrast to the pure transition to the ground state, the gamma rays leading to the first excited state may often show an angular distribution produced by a mixed transition. The mixing ratio, and consequently the angular distribution, can vary widely. Whenever the ground-state transition is not observed, therefore, any spin assignment based on the angular distribution of the gamma ray to the first excited state alone has to be considered with great care. Of the ten resonances studied here, four did not show any observable ground-state transition. In each of these cases, the ratio $\Gamma_{\gamma 0}/\Gamma_{\gamma 1}$ has an upper limit of 1/10. It is therefore very unlikely that they are either 1^- or 2^+ states.

A 3^- state in Si^{28} can decay to the first excited state by an $E1$ and $M2$ mixture. Although the $M2$ admixture is expected to be very small, an admixture of about 1% $M2$ can change the anisotropic $E1$ distribution into an isotropic one simulating the distribution of a 0^+ state. However, no small admixture can produce the distribution expected for a 4^+ compound state; so if the latter distribution is observed, a 4^+ state is indicated. This ambiguity between the obvious 0^+ state and a 3^- state with $M2$ admixture can be resolved in some cases by a study of the elastically scattered particles.

The elastic scattering of alpha particles by a zero-

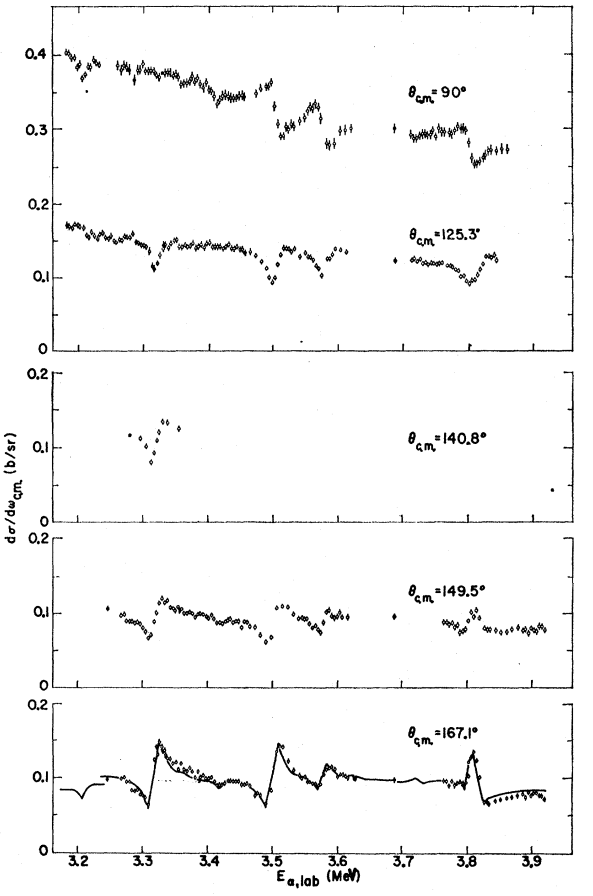

FIG. 6. Yield of elastically-scattered alpha particles from alpha-particle bombardment of Mg^{24}, plotted as a function of alpha-particle energy. The angle of observation is indicated for each curve. The target was 13 keV thick to 3.5-MeV alpha particles.

[10] J. R. Cameron, Phys. Rev. **90**, 839 (1953).
[11] J. A. Weinman, Nucl. Instr. Methods **18**, 777 (1963).
[12] M. E. Rose, Phys. Rev. **91**, 610 (1953).

spin nucleus has been discussed by several authors.[10] The differential cross section includes sums over the partial waves for the different angular momenta involved in the reaction. Since each partial wave includes a Legendre polynomial as a factor, angles of observation were chosen to correspond to zeros of these polynomials. Then if partial waves with $l_\alpha > 4$ are excluded from consideration, the spins and parities of the observed resonances could easily be determined from the following criteria.

(1) All resonances will be observed at the most backward angle $\theta_{c.m.} = 167.1°$.

(2) A $J = 0^+ (l_\alpha = 0)$ resonance will appear at all angles with equal intensity.

(3) A $J = 1^- (l_\alpha = 1)$ resonance will appear at all angles except $\theta_{c.m.} = 90°$.

(4) A $J = 2^+ (l_\alpha = 2)$ resonance will appear at all angles except $\theta_{c.m.} = 125.3°$. In our work, d-wave resonances accidentally exhibit a weak interference pattern at 167.1° whenever $\Gamma_\alpha/\Gamma \gtrsim 0.8$.

(5) A $J = 3^- (l_\alpha = 3)$ resonance will appear at all angles except $\theta_{c.m.} = 90°$ and $\theta_{c.m.} = 140.8°$.

(6) A $J = 4^+ (l_\alpha = 4)$ resonance will appear at all angles except $\theta_{c.m.} = 149.5°$.

In this experiment, the counters were set at the zeros of the Legendre polynomials ($\theta_{c.m.} = 90°$, 125.3°, 140.8°, and 149.5°) and at 167.1°. The widths and shapes of the observed resonances were fitted by use of the graphical method discussed in Refs. 10 and 11. Although the observed widths of all narrow resonances are entirely due to the 13-keV target thickness, the widths of broader resonances could be extracted from the measurements by use of the procedure described in Ref. 11. These widths could be compared with the total widths observed in the (α,γ) thick-target yield (Table I). This comparison allows a rough estimate[11] of the ratio Γ_α/Γ.

Parameters for the observed resonance levels in Si^{28} have been assigned by the methods outlined above and are summarized in Table I. These assignments are discussed in more specific detail below.

A. The 2^+ Resonances

The prominent resonances observed at $E_\alpha = 3.206$, 3.418, 3.661, and 4.35 MeV can all be assigned spin and parity 2^+. As illustrated in Fig. 5, the angular distributions of the ground-state transitions are all fitted by the predicted curve for a 2^+ state and by no other. Except for the 3.418-MeV resonance, the value $(2I+1)\Gamma_\alpha\Gamma_{\gamma 1}/\Gamma$ is computed on the assumption that the gamma ray to the first excited state has an isotropic angular distribution.

As can be seen from Table I, the values of $(2I+1)\Gamma_\alpha\Gamma_{\gamma 0}/\Gamma$ or $(2I+1)\Gamma_\alpha\Gamma_{\gamma 1}/\Gamma$ are larger for the 2^+ resonances than for any others; at the 3.21-MeV resonance both γ-ray transitions are strong. Since rough estimates of the ratio Γ_α/Γ are available for all these resonances except the 4.35-MeV one, gamma-ray widths Γ_γ can be derived. They are listed in Table I together with the theoretical single-particle gamma-ray widths.[13] A comparison of the two values for each 2^+ resonance shows that at least one of the two electric-quadrupole transitions has a strength equal to about one full Weisskopf unit.

In contrast to the (α,γ) reaction, the elastic α scattering in Mg^{24} gives only poor evidence of the 2^+ states in Si^{28}. By accident these states exhibit a very weak interference pattern, as can be seen in Fig. 6. The parameters for the 3.213-MeV resonance listed in Table I are in very good agreement with the values measured in earlier work.[5]

B. The 0^+ Resonances

These resonances show gamma-ray transitions only to the first excited state. Therefore a unique spin assignment cannot be made on the basis of the isotropic angular distribution of the gamma rays leading to the 1.78-MeV excited state; as mentioned above, a 3^- state can also exhibit an isotropic distribution if the gamma-ray transition is electric dipole with an admixture of a few percent magnetic quadrupole. In the two resonances at 3.583 and 3.807 MeV, this ambiguity could be removed by observing the elastically scattered α particles. The fact that in both cases the interference pattern can be seen at all angles indicates a 0^+ resonance. [The agreement of the measured total width in the (α,γ) reaction with that in the (α,α) gives assurance that the same resonance is studied in both cases.] Again the ratio $\Gamma_\alpha/\Gamma_{\text{total}}$ could be estimated and the widths Γ_γ could be derived. The strengths of these electric-quadrupole transitions are only about a quarter of the Weisskopf estimates. A third resonance at 3.307 MeV shows an isotropic angular distribution for the gamma rays leading to the first excited state and has no ground-state transitions. This suggests that possibly it is a 0^+ resonance. Here the elastic α-particle scattering does not exhibit an observable interference pattern, perhaps because the total width of the state is too much smaller than the target thickness. The spin assignment therefore remains ambiguous. The small width of this state could well indicate a 3^- state.

C. The 4^+ Resonance

Our only 4^+ resonance, the one at 3.363 MeV, is probably the state seen in the (p,α) work.[3] A comparison of the values $(2I+1)\Gamma_p\Gamma_\alpha/\Gamma$ and $(2I+1)\Gamma_\alpha\Gamma_\gamma/\Gamma$ shows that the ratio Γ_p/Γ_γ is of the order of 350. (In both cases only the α-particle widths to the ground-state are considered.) The small width of the state again prevents observation of the elastic scattering of α particles.

[13] V. F. Weisskopf, Phys. Rev. **83**, 1073 (1951).

D. The 1^- Resonances

Both of the 1^- states, observed at 3.318 and 3.504 MeV in the (α,γ) work, show the angular distribution uniquely characteristic of an electric-dipole γ ray to the ground state. This allows an unambiguous spin assignment. The elastically-scattered α particles exhibit a 1^- interference pattern only for the 3.318-MeV state; the scattering of the 3.504-MeV resonance is perturbed by a nearby 0^+ resonance. The ratio Γ_α/Γ, which therefore can be only estimated for the 3.318-MeV state, leads to a radiation width $\Gamma_\gamma \approx 0.15$ eV. This value is only about 10^{-4} of the Weisskopf estimate. It is known that electric-dipole transitions in self-conjugate nuclei are strongly inhibited whenever the isotopic spin remains unchanged in the transitions. We therefore conclude that the state that corresponds to the 3.318-MeV resonance has isotopic spin $T=0$.

VI. COMPARISON WITH EARLIER WORK

Some of our results from the $Mg(\alpha,\gamma)$ and $Mg(\alpha,\alpha)$ work can be compared with those of other authors. The resonance at $E\alpha = 3.21$ MeV, as mentioned above, was also studied by Smulders and Endt[5] in the α-capture process. Good agreement is obtained for all the different values listed in Table I.

All other resonances up to $E_\alpha = 3.45$ MeV can be compared with the $Al^{27}(p,\gamma)$ and $Al^{27}(p,\alpha)$ reactions measured by Anderson *et al.*[2,3] Their results for the total width, spin, parity, and the quantity $(2I+1)\Gamma_p\Gamma_\alpha/\Gamma$ are shown in Table I. For energies $E_\alpha > 3.45$ MeV, the quantity $(2I+1)\Gamma_p\Gamma_\alpha/\Gamma$ can be only estimated for resonances with isotropic angular distribution by using the data of Kaufmann *et al.*[4] These authors, who observed at a fixed angle over the energy range $3.2 < E_\alpha(\text{lab}) < 3.9$ MeV, measured the relative yield of the $Al^{27}(p,\alpha)Mg^{24}$ reaction leading to the ground state of Mg^{24}. At the lower energies, some of their resonances overlap the data of Ref. 3 so that the relative yield with isotropic angular distribution can be calibrated in terms of $(2I+1)\Gamma_p\Gamma_\alpha/\Gamma$. Where two resonances are unresolved [e.g., at $E_\alpha(\text{lab}) = 3.504$ MeV], only an upper bound to this quantity could be assigned by assuming that the α yield was attributable entirely to the resonance $I^\pi = 0^+$. These estimated values of $(2I+1)\Gamma_p\Gamma_\alpha/\Gamma$ are also shown in Table I.

Anderson *et al.*[3] have given definite spin and parity assignments for 3 of our resonances, namely those at $E_\alpha = 3.21$, 3.36, and 3.42 MeV. Here not only their values of spin and parity but also those of the total width agree well with ours. We therefore can be sure that these three resonances can be seen in all four reactions. Clearly we have not seen the resonance at $E_\alpha = 3.45$ MeV which is listed as having either the assignment 3^- or 2^+, and for which the value $(2I+1) \times \Gamma_p\Gamma_\gamma/\Gamma = 50$ eV is given in the summary by Endt and van der Leun.[2] Combining this value with the ones stated in Table I and taking $\Gamma = \Gamma_p + \Gamma_\alpha$ shows that $(2I+1)\Gamma_\alpha\Gamma_\gamma/\Gamma \gg 1$ eV. In our work the lower limit for $(2I+1)\Gamma_\alpha\Gamma_\gamma/\Gamma$ is about 0.02 eV. Therefore we definitely should have seen this resonance. The fact that we did not observe it indicates that the resonance seen in the (p,γ) work is not the same one seen in the (p,α) reaction. In the alpha-scattering experiment, we cannot observe this resonance because its width is too narrow for the target thickness we used. Two more resonances close to the ones we saw at $E_\alpha = 3.32$ MeV and at $E_\alpha \approx 3.25$ MeV were measured by Anderson *et al.* but not observed by us.

ACKNOWLEDGMENTS

The authors are pleased to thank the members of the Argonne Van de Graaff group for their skillful operation of the accelerator. We are particularly indebted to John McShane for his help in construction and maintenance of the low-carbon target system. We also wish to thank Dr. P. J. M. Smulders and Dr. Rolf Nordhagen for communicating results prior to publication.